

Photon shielding competence of concrete doped CuO for gamma shielding applications

Salisu Hudu¹, Idris M. Mustapha^{1*}, Sulayman M. Bello², Abdullahi S. Halimatu³,
Iwa S. James⁴, Abdullahi A. Aisha⁵, and Ahmad Ubaidullah⁶

¹Department of Physics, Faculty of Natural and Applied Sciences, Nasarawa State University Keffi, Nigeria

²Department of Mathematics, Faculty of Natural and Applied Sciences, Nasarawa State University Keffi, Nigeria

³Department of Biochemistry and Molecular Biology, Faculty of Natural and Applied Sciences, Nasarawa State University Keffi, Nigeria

⁴Department of Physics, Faculty of Science, Federal University of Technology Owerri, Imo State, Nigeria

⁵Department of Physics, Joseph Sarwuan Tarka University, Makurdi, Benue State, Nigeria

⁶Department of Geophysics, Faculty of Physical Sciences, Federal University Dutsinma, Katsina State

E-mail : idrismustapham@nsuk.edu.ng

Received 21 November 2023, Revised 10 March 2024, Published 30 March 2024

Abstract: In this study, photon attenuation parameters of concrete doped CuO, were determined and their application as shielding material were discussed. The WinXCOM software was used to determine the mass attenuation coefficient (MAC) of the concrete doped CuO samples (0, 20, 40 60 and 100 wt% CuO content) for the energy range (0.015-15MeV). The linear attenuation coefficient, half value layer (HVL), mean free path (MFP), and effective atomic number (Z_{eff}) were calculated from the MAC values. The MAC values of the samples decreases rapidly up to 0.12 MeV, and beyond 0.12 MeV, Compton scattering becomes effective at intermediate energies. The LAC value vary with energy in similar way as MAC. The calculated HVL and MFP were observe to decline as the CuO doping of the glasses increased which accounts for the three photon interaction mechanisms effectiveness in the variation of HVL and MFP values with energy. The Z_{eff} shows minimal variation as the energy increases in all the concrete doped CuO samples. It can be concluded that doping CuO with concrete can greatly enhance the gamma shielding ability of the sample.

Keyword : WinXCOM software, mass attenuation coefficient, gamma radiation and radiation shielding.

1. Introduction

Radiation shielding serves a number of functions; foremost among these is reducing the radiation exposure to persons in the vicinity of radiation sources. Shielding used for this purpose is named biological shielding (Kavun et al., 2023)(Alalawi et al., 2020; Eskalen et al., 2020). Shields are used in reactors to reduce the intensity of γ -rays

incident on the reactor vessel, which protects the vessel from excessive heating due to γ -ray absorption and reduces radiation damage due to neutrons (Eskalen et al., 2020; Mustapha et al., 2021). These shields are named thermal shields. Sometimes shields are used to protect delicate electronic apparatus that otherwise would not function properly in a radiation shield. Such apparatus shields are used, for example, in some types of military equipment (Kavaz et al., 2020; Kazemi et al., 2019).

In different areas of ionizing radiation application, neutrons and photons (gamma rays) are of major concern to nuclear engineers when designing radiation shield. This is due to their abilities to penetrate deeper into any given medium (Kure, 2021). Traditionally, materials for photon attenuation are required to be of high density; on the other hand, fast neutron shields require low density hydrogenous materials as moderators. Materials rich in elements such as (B, Eu, Pu, Cd) that have high neutron absorption cross-section (Afiq et al., 2022; Sayyed et al., 2021).

A very inexpensive building material, concrete, is one of the primary elements found in nuclear radiation installations. In order to provide concrete doped metal oxide materials with improved characteristics for radiation shielding applications, ongoing research is being conducted. (Afiq et al., 2022). This would lead to a reduction in the needed thickness/area, simplifying the overall design requirements, and saving materials, thus decreasing the total costs. Concrete has been used in the construction of nuclear power plants since before 1975 (Kazemi et al., 2019; Kilicoglu & Tekin, 2019). It has certain advantages, such as low permeability to protect embedded steel reinforcement, durability against fire, ubiquitous materials for forming concrete, and flexibility to form any molded shapes. Concrete is mostly constructed as a protection dome in the primary containment, which contains the ionizing facility, and also in the secondary containment, which houses the turbine. It is also used to construct dry cask storage, which stores spent nuclear fuel to prevent nuclear waste contamination (Al-hadeethi et al., 2020; Alalawi et al., 2020; Kilicoglu & Tekin, 2019).

Concrete is also used to construct trenches and shielding boxes of “hot cells” for managing radioactive waste in India. This type of concrete is classified as radiation shielding concrete (RSC). RSC, also known as atomic energy protection concrete or heavyweight concrete (concrete made with magnetite aggregates can have a density of 3.2–4 t/m³, which is much higher than that of concrete made with ordinary aggregates), is a cement-based composite prepared with water, cement, and heavy weight aggregate (Farooq et al., 2012; Kavun et al., 2023; Kilicoglu & Tekin, 2019). The main purpose of the RSC design is to shield against neutrons and gamma rays. The aim of this study is to investigate the radiation shielding capabilities of concrete doped CuO for nuclear shielding application.

2. Materials and Methods

In this study, gamma attenuation parameters of concrete doped CuO of various mixing ratio of CuO content consisting of 0%, 20%, 40%, 60%, and 100% mol, were determined and their application as shielding material were discussed. Theoretical mass attenuation coefficients (MAC) of the glass mixtures were calculated for the

chemical composition of the concrete doped CuO mixtures using winXCOM software. The XCOM code is a database for calculating mass attenuation coefficients at different photon energies.

The term of mass attenuation coefficient for selected sample is expressed using following Lambert-Beer law (Al-ghamdi et al., 2022),

$$I = I_0 e^{-(\mu/\rho)t} \quad (1)$$

where I and I_0 are the intensity with absorber and intensity without absorber, respectively. t in g/cm^2 , is the thickness of the sample and μ in cm^2/g , is the mass attenuation coefficient. In addition, the MAC values of the cement doped CuO samples under study were also obtained (Mustapha et al., 2021).

The mean free path (MFP) is the average distance taken by moving particle between two consecutive collision. MFP values can be obtained by the following equation;

$$MFP = \frac{1}{\mu} \quad (2)$$

Half value of layer (HVL) of the materials is the thickness which reduce the incident photon intensity to fifty percent. The equation (3) is utilized to determine the HVL for the material (Mustapha et al., 2021).

$$HVL = \frac{0.693}{\mu} \quad (3)$$

where μ (cm^{-1}) denotes linear attenuation coefficient which is determined by the multiplication of the MAC value and density of the sample (ρ) (Kavaz et al., 2020).

The Z_{eff} values of materials have a strong energy dependence, which differs from the Z (atomic number) of individual elements (for example, Z is constant with changing E). In this study, the equations 4 was used to calculate the Z_{eff} of the investigated glasses mixtures

$$Z_{\text{eff}} = \frac{\sum f_i A_i \left(\frac{\mu}{\rho}\right)_i}{\sum f_j A_j \left(\frac{\mu}{\rho}\right)_j} \quad (4)$$

where Z_i , f_i , and A_i , are the atomic number, molar fraction, and atomic mass of the elements inside the samples, respectively (Eskalen et al., 2020; Kavaz et al., 2020).

3. Results and Discussion

The molar volume and density of the concrete doped CuO were shown in Table 1. The densities of the samples were varied depending on the proportion of additives (CuO). The density and molar volume of samples are increased with increment in CuO percentage. The high density of a material is important not only for the attenuation of photon radiation, but also for reducing the thickness of the shielding material.

The mass attenuation coefficient (MAC) of the samples were measured for 0.015-15 MeV photon energies theoretically by using WinXCOM program shown in Table 2. The result shows the highest and lowest attenuation coefficient in pure CuO sample (S5) and pure concrete sample (S1) respectively. The value attenuation coefficient increases with increasing CuO concentration in all the samples. It is obvious that the values of attenuation coefficient depend on both photon energy and chemical composition of samples. In low energy region, since photoelectric cross section changes proportional

with Z^4 and inversely proportional with the incident photon energy as $E^{3.5}$. Mass attenuation values of the samples were decreased rapidly up to 0.12 MeV. Beyond 0.12 MeV, Compton scattering becomes effective at intermediate energies. Mass attenuation values of the samples are almost constant and zero due to the linear dependence of cross-section of Compton scattering with atomic number Z .

The linear attenuation coefficient (LAC) was calculated from MAC and the density of the samples as a function of energy as depicted in Fig. 2. The LAC vary with energy in similar way as MAC. The increase in density of the samples greatly affect the attenuation capability.

Table 1. Chemical compositions and densities of the Concrete doped CuO

S/n	Sample Code	Concentrate	CuO	Density
1.	S1	100	0	2.34
2.	S2	80	20	2.53
3.	S3	60	40	2.79
4.	S4	40	40	2.93
5.	S5	0	100	3.11

Table 2. Mass Attenuation Coefficient of the investigated Concrete doped CuO in the range (0.015-15)MeV.

Energy	S1	S2	S3	S4	S5
0.015	5.9600	16.700	27.4000	38.1000	59.5000
0.02	2.6700	7.5700	12.5000	17.4000	27.2000
0.03	0.9360	2.5100	4.0800	5.6500	8.7900
0.04	0.5040	1.1900	1.8800	2.5600	3.9400
0.05	0.3470	0.7040	1.0600	1.4200	2.1300
0.06	0.2750	0.4820	0.6890	0.8960	1.3100
0.07	0.2350	0.3660	0.4960	0.6260	0.8860
0.08	0.2120	0.2980	0.3840	0.4710	0.6430
0.09	0.1960	0.2560	0.3150	0.3750	0.4940
0.10	0.1840	0.2270	0.2700	0.3120	0.3970
0.20	0.1380	0.1400	0.1420	0.1450	0.1490
0.30	0.1180	0.1170	0.1150	0.1140	0.1110
0.40	0.1050	0.1030	0.1010	0.0988	0.0944
0.50	0.0961	0.0937	0.0914	0.0890	0.0844
0.60	0.0888	0.0864	0.0841	0.0818	0.0771
0.70	0.0828	0.0806	0.0783	0.0761	0.0716
0.80	0.0779	0.0757	0.0735	0.0714	0.0670
0.90	0.0737	0.0716	0.0695	0.0674	0.0632
1.00	0.0700	0.0680	0.0660	0.0640	0.0600
1.50	0.0570	0.0553	0.0537	0.0521	0.0488
2.00	0.0490	0.0477	0.0464	0.0451	0.0426
3.00	0.0396	0.0389	0.0381	0.0374	0.0360
5.00	0.0306	0.0307	0.0308	0.0308	0.0310

Energy	S1	S2	S3	S4	S5
7.00	0.0264	0.0270	0.0276	0.0282	0.0294
9.00	0.0240	0.0250	0.0260	0.0270	0.0290
11.00	0.0225	0.0238	0.0251	0.0264	0.0291
13.00	0.0215	0.0230	0.0246	0.0262	0.0293
15.00	0.0208	0.0226	0.0243	0.0261	0.0297

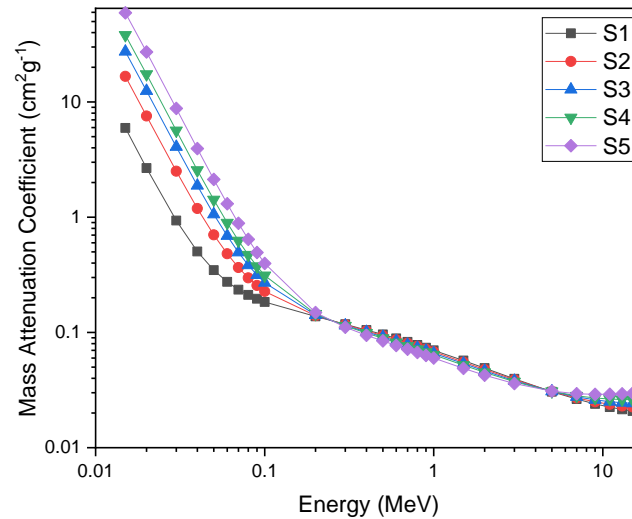


Fig. 1. Mass attenuation coefficient spectra of the concrete doped CuO samples.

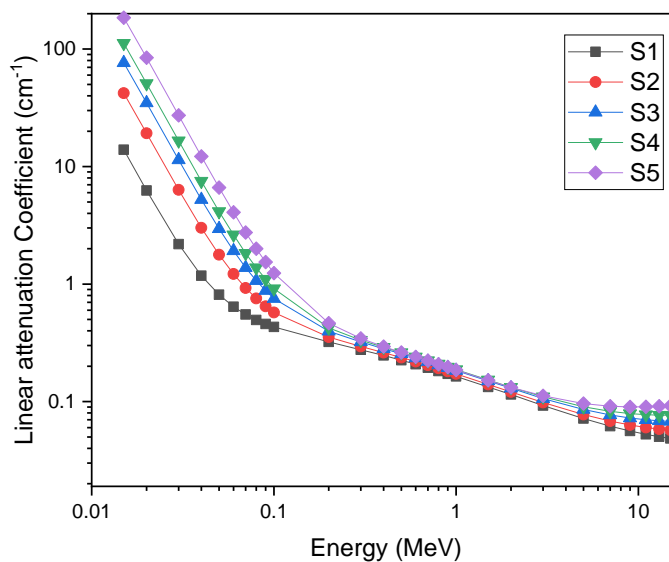


Fig. 2. Linear attenuation coefficient spectra of the concrete doped CuO samples.

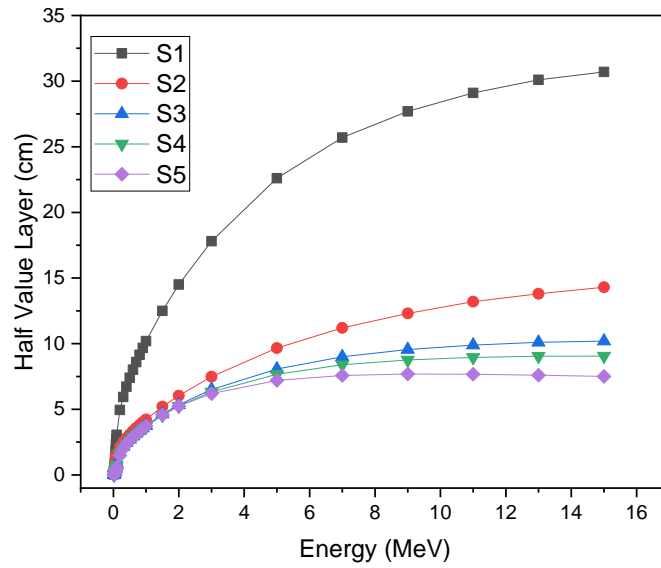


Fig. 3. Half Value Layer of the concrete doped CuO samples.

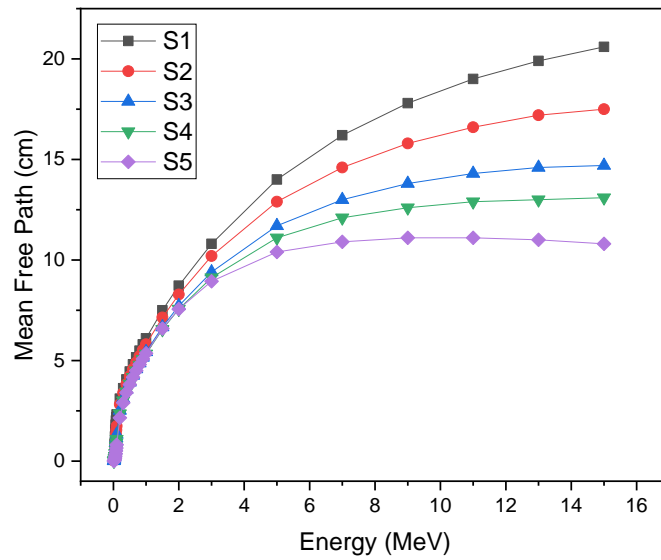


Fig. 4. Mean Free Path of the concrete doped CuO samples.

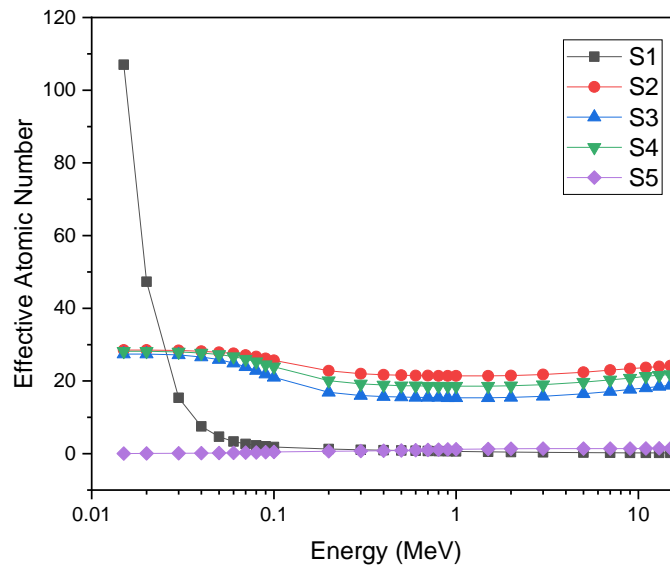


Fig. 5. Effective atomic number of the concrete doped CuO samples.

The half value layer (HVL) and mean free path (MFP) enables us to obtain in an easy way a material’s shielding ability. Figure 3 and 4 represents HVL and MFP values versus the incident photon energy for 0.015-15 MeV. In contrast to LAC values, HVL values are enhanced as the photon energy increases, respectively. The HVL and MFP values also depend on the density of the sample in inverse proportion. Pure CuO sample have smaller values comparing with other samples due to its higher density in both HVL and MFP. Firstly, values of HVL were raised with increment in photon energy up to 2 MeV, then tended to rise slowly and remain stable. At low energies, HVL is less dependent from the content of the material.

A vital parameter to consider a material to be substituted for radiation shielding is the effective atomic number (Z_{eff}). The fluctuation of Z_{eff} with respect to photon energy is depicted in Fig. 5. The Z_{eff} of the samples shows a near constants value with negligible variation for all the concrete doped CuO samples. The Pure concrete sample shows a drastic fall in Z_{eff} value to an energy of 0.04 MeV and flattens out for higher energy. The lower Z_{eff} values were found in low and high energy region for all samples. The addition of CuO in concrete systems is responsible for the increase in Z_{eff} values

4. Conclusion

This study is aimed to investigate gamma ray shielding parameters of concrete doped CuO samples theoretically using WinXCOM software. The mass attenuation coefficient, linear attenuation coefficient, half value layer, mean free path and effective atomic number, which are the significant gamma attenuation parameters were obtained theoretically for 0.015 – 15 MeV photon energies. The highest MAC and LAC values were observed at 0.015 MeV, i.e. low energies, for all the samples. In contrast to LAC values, HVL values are enhanced as the photon energy increases, respectively. The

HVL and MFP values also depend on the density of the sample in inverse proportion. The Z_{eff} of the samples shows a near constants value with negligible variation for all the concrete doped CuO samples. The Pure concrete sample shows a drastic fall in Z_{eff} value to an energy of 0.04 MeV and flattens out for higher energy. The outcomes indicate that the insertion of CuO into concrete enhanced the photon shielding parameters. It can be concluded that CuO doped concrete samples can be further evaluated for gamma protection applications.

References

- Afiq, M., Abdullah, H., Saifulnaz, R., Rashid, M., Amran, M., Hejazii, F., Azreen, N. M., Fediuk, R., Voo, Y. L., Vatin, N. I., & Idris, M. I. (2022). Recent Trends in Advanced Radiation Shielding Concrete for Construction of Facilities: Materials and Properties. *Journal of Polymers*, *14*(1–47).
- Al-ghamdi, H., Elsafi, M., Almuqrin, A. H., & Yasmin, S. (2022). Investigation of the Gamma-ray Shielding Performance of CuO-CdO-Bi₂O₃ Bentonite Ceramics Hanan. *Journal of Materialss*, *15*, 1–12.
- Al-hadeethi, Y., Sayyed, M. I., & Al-buriah, M. S. (2020). Bioactive glasses doped with TiO₂ and their potential use in radiation shielding applications. *Ceramics International*, *February*, 0–1. <https://doi.org/10.1016/j.ceramint.2020.02.276>
- Alalawi, A., Al-buriah, M. S., & Rammah, Y. S. (2020). Radiation shielding properties of PNCKM bioactive glasses at nuclear medicine energies. *Ceramics International*, *March*, 1–7. <https://doi.org/10.1016/j.ceramint.2020.03.033>
- Eskalen, H., Kavun, Y., Kerli, S., & Eken, S. (2020). An investigation of radiation shielding properties of boron doped ZnO thin films. *Journal of Optical Materials*, *105*(March), 109871. <https://doi.org/10.1016/j.optmat.2020.109871>
- Farooq, I., Imran, Z., Farooq, U., Leghari, A., & Ali, H. (2012). *Bioactive Glass : A Material for the Future Bioactive Glass : A Material for the Future*. May 2014. <https://doi.org/10.5005/jp-journals-10015-1156>
- Kavaz, E., Armoosh, S. R., Peri, U., Ahmadi, N., & Oltulu, M. (2020). Gamma ray shielding e ff ectiveness of the Portland cement pastes doped with brass-copper : An experimental study. *Journal of Radiation Physics and Chemistry*, *166*(July 2019). <https://doi.org/10.1016/j.radphyschem.2019.108526>
- Kavun, Y., Eskalen, H., & Kavgacı, M. (2023). A study on gamma radiation shielding performance and characterization of graphitic carbon nitride. *Journal of Chemical Physics Letters*, *811*(140246). <https://doi.org/10.1016/j.cplett.2022.140246>
- Kazemi, F., Malekie, S., Science, N., & Hosseini, M. A. (2019). *A Monte Carlo study on the Shielding Properties of a Novel Polyvinyl Alcohol (PVA)/WO₃ Composite, against gamma rays, using the MCNPX Code*. August. <https://doi.org/10.31661/jbpe.v0i0.1114>
- Kilicoglu, O., & Tekin, H. O. (2019). Bioactive glasses and direct e ff ect of increased K₂O additive for nuclear shielding performance: A comparative investigation. *Ceramics International*, *September*, 0–1. <https://doi.org/10.1016/j.ceramint.2019.09.095>

- Kure, O. I. O. M. M. I. M. (2021). *Photon and Fast Neutron Transmission Parameters of Metakaolin Doped Concrete*. 03(02), 58–66.
- Mustapha, I. M., James, A. B., & Bello, S. M. (2021). Photon Shielding Characterization of SiO₂-PbO-CdO-TiO₂ Glasses for Radiotherapy Shielding Application. *Asian Journal of Research and Reviews in Physics*, 4(4), 32–38. <https://doi.org/10.9734/ajr2p/2021/v4i430150>
- Sayyed, M. I., Almuqrin, A. H., Kumar, A., & Jecong, J. F. M. (2021). Optik Optical , mechanical properties of TeO₂-CdO-PbO-B₂O₃ glass systems and radiation shielding investigation using EPICS2017 library. *Optik*, 242(June), 167342. <https://doi.org/10.1016/j.ijleo.2021.167342>.